Texture Feature Variability in Ultrasound Video of the Atherosclerotic Carotid Plaque

CHRISTOS P. LOIZOU[ID][1], **(Senior Member, IEEE),**
CONSTANTINOS S. PATTICHIS[2], **(Senior Member, IEEE), MARIOS PANTZIARIS**[3],
EFTHYVOULOS KYRIACOU[4], **(Senior Member, IEEE), AND ANDREW NICOLAIDES**[5]

[1] Department of Electrical, Computer Engineering and Informatics, Cyprus University of Technology, 3036 Limassol, Cyprus
[2] Department of Computer Science, University of Cyprus, 1678 Nicosia, Cyprus
[3] Institute of Neurology and Genetics, 1683 Nicosia, Cyprus
[4] Department of Computer Science and Engineering, Frederick University, 3080 Limassol, Cyprus
[5] Cyprus Cardiovascular Disease Educational Research Trust, 2368 Nicosia, Cyprus
CORRESPONDING AUTHOR: C. P. LOIZOU (panloicy@logosnet.cy.net)

ABSTRACT The objective of this paper was to investigate texture feature variability in ultrasound video of the carotid artery during the cardiac cycle in an attempt to define new discriminatory biomarkers of the vulnerable plaque. More specifically, in this paper, 120 longitudinal ultrasound videos, acquired from 40 normal (N) subjects from the common carotid artery and 40 asymptomatic (A) and 40 symptomatic (S) subjects from the proximal internal carotid artery were investigated. The videos were intensity normalized and despeckled, and the intima-media complex (IMC) (from the N subjects) and the atherosclerotic carotid plaques (from the A and S subjects) were segmented from each video, in order to extract the M-mode image, and the texture features associated with cardiac states of systole and diastole. The main results of this paper can be summarized as follows: 1) texture features varied significantly throughout the cardiac cycle with significant differences identified between the cardiac systolic and cardiac diastolic states; 2) gray scale median was significantly higher at cardiac systole versus diastole for the N, A, and S groups investigated; 3) plaque texture features extracted during the cardiac cycle at the systolic and diastolic states were statistically significantly different between A and S subjects (and can thus be used to discriminate between A and S subjects successfully). The combination of systolic and diastolic features yields better performance than those alone. It is anticipated that the proposed system may aid the physician in clinical practice in classifying between N, A, and S subjects using texture features extracted from ultrasound videos of IMC and carotid artery plaque. However, further evaluation has to be carried out with more videos and additional features.

INDEX TERMS Ultrasound video, texture analysis, carotid plaque, texture variability, cardiovascular disease.

I. INTRODUCTION

There are indications that the structure and morphology of the atherosclerotic carotid plaque recorded from ultrasound video have prognostic implications [1] and their detection may improve risk prediction [2]. Traditionally, the degree of stenosis in the carotid artery was used to predict the risk of stroke [3] but it was shown not to be very reliable in many cases. There are numerous studies that indicated that image based markers may provide a more reliable information in predicting stroke risk compared to stenosis measurements [3], [4]. Ultrasound video of the carotid artery is now widely used and has further improved the outcome of the diagnosis of the arterial disease [3], [4]. Furthermore, it was shown that texture features extracted from ultrasound imaging of the atherosclerotic carotid plaque may provide additional information to the physician for assessing stroke risk and consequently stroke treatment, thus improving patient management [3]–[6]. Furthermore, it was suggested in [7], that spatial distributions of gray levels in the tissue under investigation, correspond to the relative distribution of echogenic (e.g. fibrous and calcified tissue) and echolucent (e.g. blood, lipids) materials and are considered to be related to the risk of stroke. Furthermore, it is noted that carotid plaque texture feature variability throughout the cardiac cycle

TABLE 1. An overview of texture feature variability studies in ultrasound video of the atherosclerotic carotid plaque.

Study	Year	Method	NR (N/A/S)	Findings
Kanber [8]	2013	Manual segmentation	-/-/47	Carotid artery diameter not correlated with GSM over the cardiac cycle. No statistical significance between systole and diastole for plaque GSM (p=0.34). GSM correlated with presence of symptoms (p=0.02).
Kanber [9]	2013	Manual segmentation	-/-/27	Neither systolic nor diastolic states were estimated for stud GSM variability. Periodic variations of GSM were recorde follows: GSM 40.5±1.69 (%CV=4.2%) vs 34.8± (%CV=5.2%).
Golemati [4]	2015	Manual segmentation	-/25/-	Found SD differences between wall and plaque for low stenosis subjects for contrast (8.56±7.98 vs 8.88±9.1 at wall) and correlation (0.07±0.05 vs 0.04±0.16 at plaque) at systole vs diastole respectively.
This study	2016	Semi-automated segmentation based on snakes	40/40/40	TF may separate N, A and S groups for both the cardiac systolic and diastolic states. For example, GSM at systole vs diastole were: 42.12±3.15 vs 39.38±2.01, p=0.001 for the N group, 44.10±1.84 vs 34.88±1.96, p=0.001 for the A group and 35.73±1.69 vs 29.01±2.25, p= 0.001 for the S group.

CVD: Cardiovascular events; N: Number of cases investigated; significantly (shown underlined) and non-significantly different at p<0.05 and p>=0.05 respectively.

corresponds to plaque deformation and compression and the pulse pressure. However, to the best of our knowledge, there is no scientific biological evidence published in the literature linking the variability of the plaque texture with risk stratification due to the carotid wall movement during the cardiac cycle.

As shown in Table 1 there are very few studies reported in the literature where texture feature variability through the cardiac cycle was investigated in ultrasound video of the carotid artery. More specifically, Kanber *et al.* [8], performed manual segmentation of the atherosclerotic carotid plaque on ultrasound videos acquired from 47 symptomatic (S) subjects and showed that the carotid artery diameter is not correlated with the gray-scale median (GSM) of the plaque, over the entire cardiac cycle. In another study by the same group [9], the GSM variability was estimated in 27 S subjects where periodic variations of the GSM were recorded at systolic and diastolic points. Moreover, Golemati *et al.* [4], performed a study on 25 low stenosis asymptomatic (A) subjects and found significant differences between wall and plaque for contrast and correlation at systolic and diastolic points.

In the present study, we propose an integrated software system for the assessment of the texture feature variability throughout the cardiac cycle (discriminating between systolic and diastolic states) in ultrasound video of the atherosclerotic carotid plaque. Furthermore, video texture feature analysis was investigated for classifying A and S subjects. The integrated software system is based on components from previous published work by our group on video segmentation of the atherosclerotic carotid plaque [10]. Preliminary results on a very small number of A and S subjects only were published in [11] and [12].

II. MATERIALS & METHODS
A. RECORDING OF ULTRASOUND VIDEOS
A total of 120 B-mode longitudinal ultrasound videos were recorded from 40 normal (N) subjects aged 38±8.5 years,

40 asymptomatic (A) subjects aged 55±11.2 years and 40 symptomatic (S) subjects (Stroke and Transient Ischemic Attack (TIA's)) aged 54±14.3 years. The total numbers of female and male subjects were 67 (N=16, A=11, S=17) and 53 (N=24, A=29, S=23) respectively. The videos acquired from the N subjects were from the common carotid artery and were free from any atherosclerotic formation. All patients were examined during routine diagnostic procedures and a written informed consent was obtained according to the instructions of the local ethics committee, while all personal data were kept confidential. The videos recorded from the A and S subjects were from the proximal internal carotid artery and had atherosclerotic carotid plaques. All videos were acquired with the ATL HDI-5000 ultrasound scanner (Advanced Technology Laboratories, Seattle, USA) and were recorded digitally at 576 × 768 pixels with 256 gray levels and a pixel size of 59 μm (17 pixels per mm). A frame rate of 100 frames per second was used and usually 800 to 2000 frames were recorded. The scan (probe) was held in a location and orientation parallel to the atherosclerotic plaque and the arterial wall with the subject holding its breath. Additional details may be found in [10]–[12]. This frame rate is high, however it was used as these videos will also be analysed for plaque motion estimation. The ATL HDI-5000 ultrasound scanner is equipped with a 256-element fine pitch high-resolution 50-mm linear array, a multi-element ultrasound scan head with an extended operating frequency range of 5–12 MHz and it offers real spatial compound imaging.

B. ULTRASOUND VIDEO NORMALIZATION
Brightness adjustments of ultrasound videos were carried out based on the method introduced in [13]. This improves image compatibility by reducing the variability introduced by different gain settings, different operators, different equipment, and facilitates ultrasound tissue comparability [13]. This is a well-accepted standardization procedure used widely. During the normalization procedure, a small homogeneous area in
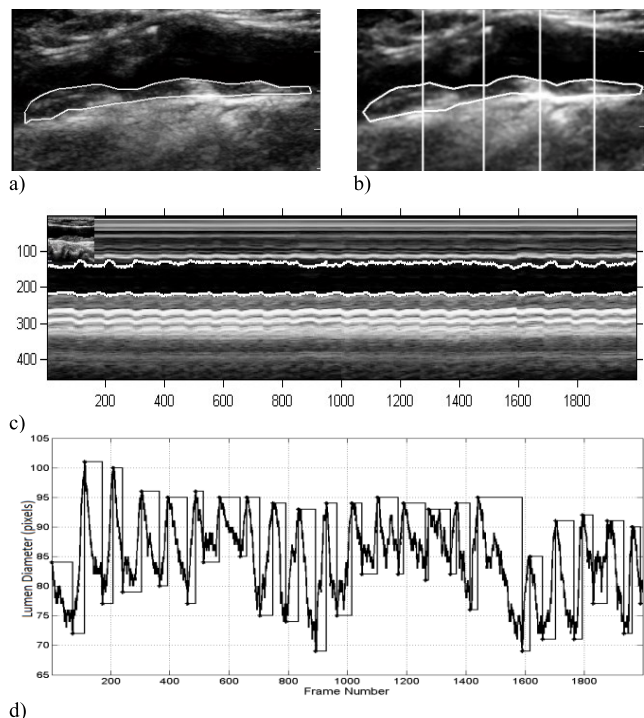
FIGURE 1. Illustration of the steps followed for segmenting the plaque, computing the M-mode image and the state diagram from a video of an asymptomatic male subject at the age of 69 with 65% stenosis. a) 200th frame of the B-mode ultrasound video (where the original image before normalisation and despeckle filtering is shown), and segmentation of the plaque at the far wall of the left carotid artery. b) 200th frame of the video after normalisation and despeckle filtering with 4 perpendicular rays selected. c) Segmented M-mode image at the far and near wall boundaries prescribed by the upper and lower white curves produced for the fourth ray in Fig. 1b. For each of the four rays an M-Mode image was produced. The M-mode image shows the dynamic variations of the near and far wall boundaries. d) Four different diameter change curves were produced from the subtraction of the near and far wall boundaries from the corresponding images produced in c). The average of the four was computed and displayed in Fig. 1d). The diagram shows cardiac systolic and cardiac diastolic video frames from 0-2000 (100 frames per second=20 seconds). The contraction and distension frames are given in the first 10 sec. Contraction frames: 72-113, 174-208, 242-304, 367-393, 461-487, 515-568, 639-659, 706-749, 793-834, 892-929. Distension frames: 114-173, 209-241, 305-366, 394-460, 488-514, 569-638, 660-705, 750-792, 835-891, 930-980. Maximum carotid diameter 9.18 mm at frame 173, Minimum carotid diameter: 7.46 mm at frame 639.

the blood area was selected and the grayscale median value of this area was estimated, which was in the range from 0-5. In the same manner, a small homogeneous area in the adventitia was selected and the grayscale median of this area was also estimated, which was in the range of 180-190. Care was taken during the normalization procedure, so that an area with the above characteristics would be selected [13]. Algebraic (linear) scaling of the first video frame was manually performed by linearly adjusting the image based on the blood and adventitia values given above. The result of this is that the intensity of the gray level values on the video frames ranged from 0-255. Thus, the brightness of all pixels in the video frame was readjusted according to the linear scale defined by selecting the two reference regions (blood and adventitia, see also Fig. 1a, b) [10]. The subsequent frames of the video were

normalised (and then despeckled, see subsection II.C) based on the selection of the first frame by using the same linear scale from the first video frame, as shown in [10]. It is noted that a key point to maintaining a high reproducibility was to ensure that the ultrasound beam was at right angles to the adventitia, adventitia was visible adjacent to the plaque and that for image normalization, a standard sample consisting of the half of the width of the brightest area of adventitia was obtained.

C. SPECKLE REDUCTION FILTERING (DSFLSMV)

For speckle reduction, the filter DsFlsmv [14], [15] (despeckle filter linear scaling mean variance) was applied to the ROI in each consecutive frame prior the intima-media complex (IMC) and plaque segmentation [16]. The filters of this type utilize first order statistics such as the variance and the mean of a pixel neighborhood and may be described with a multiplicative noise model [14] by the following equation:

$$f_{i,j} = \bar{g} + k_{i,j}\left(g_{i,j} - \bar{g}\right) \tag{1}$$

where $f_{i,j}$, is the estimated noise-free pixel value, $g_{i,j}$, is the noisy pixel value in the moving window, $\bar{g}$, is the local mean value of an $N_1 \times N_2$ region surrounding and including pixel $g_{i,j}$, $k_{i,j}$ is a weighting factor, with $k \in [0, 1]$, and i, j are the pixel coordinates. The factor $k_{i,j}$, is a function of the local statistics in a moving window and is defined [14], [15] as:

$$k_{i,j} = \frac{(1 - \bar{g}^2\sigma^2)}{\sigma^2 + \sigma_n^2} \tag{2}$$

The values σ^2, and σ_n^2, represent the variance in the moving window and the variance of the noise in the whole video frame respectively. The moving window size for the despeckle filter DsFlsmv was 5×5 and the number of iterations applied to each video frame was two, where a complete description of the filter and its parameters can be found in [14]–[16]. An example of the application of the DsFlsmv filter is shown in Fig. 1b) after image normalisation.

D. VIDEO SEGMENTATION OF PLAQUE

The initial contour of the plaque was identified manually in the first video frame by using the first semi-automated initialization procedure as described in [10], which places the initial segmentation as close as possible to the plaque borders. The contour was then deformed using the integrated segmentation system proposed in [10] in order to estimate the plaque borders. The final plaque contour resulting from the snake deformation is mapped from the first video frame to the second frame and was sampled to provide the initialization for the snake deformation. The semi-automated segmentation was carried out for the entire video (see Fig. 1a) and Fig. 1b). Every 20 video frames the entire initialization procedure was repeated in order to detect the plaque borders again, repositioning the snake and reassuring that the snake contour would not converge away from the area of interest (see Fig. 1a) and 1b). All further additional details about the

method as well as detailed steps of the video segmentation method may be found in [10].

E. M-MODE GENERATION AND STATE IDENTIFICATION

The M-mode image [10], [16], which illustrates the dynamic variations of the artery throughout the cardiac cycle, for each video (see Fig. 1c) can be generated in such a way that it crosses all plaque borders. Perpendicular lines that cross the major axis of the plaque (from Fig. 1b), were placed automatically at the major axis quintiles (20%, 40%, 60%, and 80%) (as shown in Fig. 1b), and four M-mode images were generated for each of the corresponding four perpendicular lines as presented in [10]. Initial near and far wall M-mode boundaries were then generated by segmenting the resulting M-Mode images using the snake segmentation algorithm, similar to the intima-media complex segmentation (also used in [17] and [18]). The diameter rate of change (the difference between the near and far wall boundaries on the M-mode image is represented by the diameter rate of change) was derived, and the diastolic and systolic diameters (plaque-lumen) of the carotid artery were calculated (see also Fig. 1c) [10]. The extracted contours for the rate of change were averaged to form the final state diagram of the video (see Fig. 1d showing final states of the video), where diastolic and systolic frames were estimated at the maxima and minima of the curve.

F. TEXTURE FEATURES ANALYSIS

Texture may provide useful information for characterizing the IMC and the atherosclerotic carotid plaque in both images [5], [6] and videos [10]–[12], [17]. Using a system developed in Matlab®software [15], [16] we extracted from each IMC and plaque region of interest (ROI) (see Fig. 1a and Fig. 1b) in every video frame, 55 different texture features, from the A and S groups, while from the N group features were extracted from the intima-media complex (IMC) area. The following texture feature groups were extracted [15], [16]: (i) Statistical features (SF-6) [19], (ii) Spatial gray level dependence matrix mean values (SGLDMm-12) [19], (iii) Spatial gray level dependence matrix range of values (SGLDMr-12) [19], (iv) Gray level difference statistics (GLDS-4) [20], (v) Neighbourhood gray tone difference matrix (NGTDM-5) [21], (vi) Statistical feature matrix (SFM-4) [22], (vii) Laws texture energy measures (LTEM-5) [22], (viii) Fractal dimension analysis (FDTA-5), (ix) Fourier power spectrum (FPS-2) [22]. Only texture features that showed significant difference between the systolic and diastolic states for the groups investigated were selected (see also Fig. 2 and Fig. 3, Table 2 and Table 3). These texture features were computed using the IDF toolbox implemented in Matlab® [23].

G. STATISTICAL ANALYSIS

The Wilcoxon rank sum test was used in order to identify if for each set of features a significance difference (SD) or not (NSD) exists between the N, A and S groups. For significance
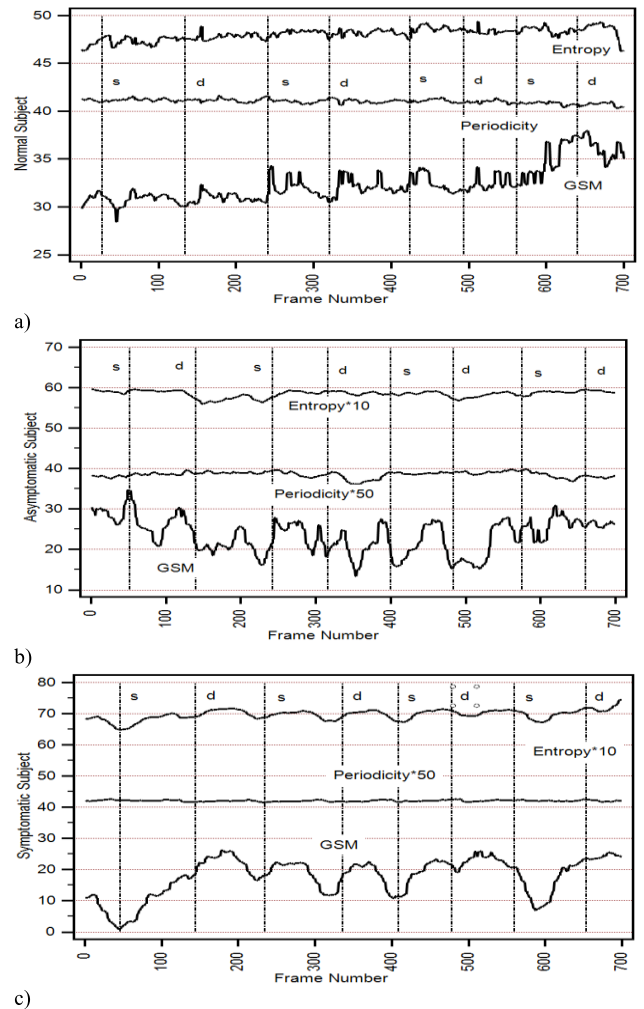

FIGURE 2. Texture feature variability through the cardiac cycle with systolic (s) and diastolic states (d) for the texture features GSM (SF), periodicity (SFM) and entropy (SGLDMr) for a) an normal (N) (male, age 38), b) an asymptomatic (A) (male, age 61) and c) a symptomatic (S) subject (male, age 63). The features for the N subject were extracted form he IMC and for the A and S subjects were extracted from the segmented plaque area (ROIs) as shown in Fig. 1a and Fig. 1b.

difference, we require p<0.05. This was done for each set of measurements for independent samples of same sizes with a confidence level of 95%. For significant differences, we require p<0.05. The coefficient of variation %CV [18], which describes the difference as a percentage of the pooled mean value with $\%CV = \frac{\sigma}{m}$, with σ, the standard deviation and m the mean value of each feature was also computed. Furthermore, box plots for different texture features between the different groups (N, A, S), were plotted. Bland–Altman plots, with 95% confidence intervals, were also used to further evaluate the difference of texture features between the groups.

H. CARDIOVASCULAR DISEASE CLASSIFICATION MODELLING

Cardiovascular disease classification modelling was used to differentiate between the A and S subjects based on the extracted texture features. Weka 3.8 workbench [24] was

TABLE 2. Selected texture features (median) that showed statistical significant difference, extracted from the IMC and plaque ROIs from 120 videos investigated for the three different groups (N, A, S). Texture features at systole (Sys) and diastole (Dia) are shown for the three different groups.

Texture Feature	Texture			%CV		
	N	A	S	N	A	S
	Sys/Dia	Sys/Dia	Sys/Dia	Sys/Dia	Sys/ Dia	Sys/Dia
Statistical Features (SF)						
GSM	42/39	44/35	36/29	3.0/3.2	4.8/ 4.6	3.0/ 3.0
STD	72/70	62/68	69/63	2.7/2.8	3.5/ 3.6	2.9/ 2.6
Spatial Gray Level Dependence Matrix (SGLDM)						
Contrast	41/19	39/26	41/29	1.7/1.9	3.5/ 3.6	2.8/2.9
Correlation	0.96/0.98	0.97/0.98	0.97/1.0	0.64/0.66	0.95/0.97	0.54/0.56
IDM	0.28/0.29	0.59/0.63	0.46/0.48	3.4/3.6	3.9/ 3.9	4.0/4.2
SV*10^3	21/22	18/21	20/31	2.1/2.3	3.2/ 3.3	2.5/2.5
Gray Level Difference Statistics (GLDS)						
Entropy	6.1/ 6.2	5.8/5.9	6.2/6.8	1.5/1.5	1.4/ 1.2	3.7/3.6
Contrast	31/28	16/13	13/10	1.7/1.3	3.5/ 3.6	2.8/2.8
Neighborhood Gray Tone Difference Statistics (NGTDM)						
Coarseness	10.1/10.2	36/39	22/25	5.8/5.8	2.5/ 2.6	6.5/6.7
Contrast	31/29	36/24	23/19	3.4/3.1	4.1/ 4.3	2.6/1.4
Statistical Feature Matrix (SFM)						
Periodicity	0.81/0.79	0.82/0.85	0.76/0.80	3.4/ 3.4	3.8/ 4.0	4.3/4.4
Roughness	2.2/2.3	2.9/2.10	2.13/2.14	4.0/4.1	2.2/ 2.1	3.3/2.2
Laws Texture Energy Measures (LTEM)						
LL*10^4	25/25	26/26	27/27	4.7/6.0	5.8/ 1.7	1.2/1.3
SS	210/221	180/169	157/165	1.3/1.3	2.1/ 2.2	2.5/2.4
Fractal Dimension Analysis (FDTA)						
H1	0.47/0.47	0.54/0.56	0.56/ 0.55	0.5/0.5	0.5/0.4	0.4/0.5

N, A, S: Normal, asymptomatic and symptomatic group of subjects, GSM: Gray scale median, STD: Standard deviation, IDM: Inverse difference moment, SV: Sum Variance, LL: Texture energy from LL kernel, SS: Texture energy from SS kernel, H1: Hoerst coefficient, %CV: Coefficient of variation.
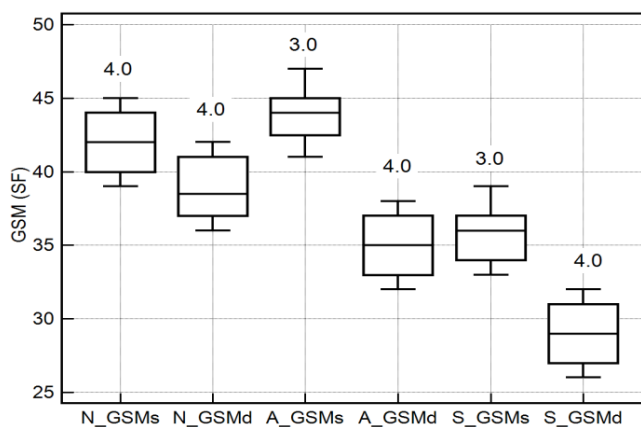

FIGURE 3. Box plots for the texture feature GSM-SF for the normal (N), asymptomatic (A) and symptomatic (S) videos for cardiac systolic (s) and cardiac diastolic (d) states extracted from the corresponding ROIs investigated in this study. Inter-quartile (±IQR) values are shown above the box plots. Straight lines connect the nearest observation with 1.5 of the IQR of the lower and upper quartiles.

used and the Support Vector Machines (SVM) [25] classifier was investigated. The SVM was trained and evaluated using 10-fold cross validation using Gaussian Radial Basis Function (RBF) kernel with a c=1 and $\gamma = 0.01$. The classifier features were selected: (i) to have statistical significant difference based on the Wilcoxon rank sum test between the 40 A and 40 S subjects for both systole and diastole as documented in Table 3, and (ii) to convey complementary information of plaque morphology. The selected features were recorded at systole (_S) and diastole (_D). These were 1: SF-GSM_S, 2: SF-GSM_D, 3: SGLDM-Contrast_S, 4: SGLDM Contrast_D, 5: GLDS-Entropy_S, 6: GLDS-Entropy_D. The performance of the classifier models was measured using the percentage of correct classifications score (%CC) based on the correctly and incorrectly classified cases and the receiver operating characteristic (ROC) metrics: true positives (TP), false positives (FP), Precision = TP/(TP+FP), Recall = TP/(TP+FN), ROC: Area under the ROC curve, mean absolute error, root mean squared error, relative absolute error, root relative squared error.

III. RESULTS

Figure 1 illustrates the 200th frame (see in Fig. 1a the original 200th frame and in Fig. 1b the normalized and despeckled 200th frame) from an ultrasound video acquired from an asymptomatic male subject at the age of 69 years old with a stenosis of 65 % and an atherosclerotic carotid plaque at the far wall of the right carotid artery. The segmented M-mode image is shown in Fig. 1c), where Fig. 1d) presents the state diagram of the video with the cardiac systolic and diastolic states over 10 cardiac cycles.

Table 2 tabulates selected texture features (median values) for the systolic and diastolic states extracted from all the

TABLE 3. Statistical analysis between the N, A, and S texture features extracted from the IMC and plaque ROI's at systole (Sys) and diastole (Dia). The Wilcoxon rank sum test was used (N vs A, N vs S, A vs S) and shown with (S) significantly and (NS) non-significantly different features at p<0.05. p-values are shown in parentheses.

Texture Feature	N vs A	N vs S	A vs S
	Sys, Dia	Sys, Dia	Sys, Dia
Statistical Features (SF)			
GSM	S(0.004), S(0.002)	S (0.01), S(0.01)	S(0.001), S(0.001)
STD	NS(0.06), NS(0.07)	NS(0.09), NS (0.06)	NS(0.71), NS(0.6)
Spatial Gray Level Dependence Matrix (SGLDM)			
Contrast	S(0.002), S(0.001)	S(0.002), S(0.001)	S(0.04), S(0.01)
Correlation	S(0.001), S(0.004)	S(0.002), S(0.002)	S(0.002), S(0.001)
IDM	S(0.003), S(0.002)	S(0.001), S(0.001)	S(0.004), S(0.001)
Sum Variance	S(0.004), S(0.001)	S(0.002), S(0.004)	S(0.002), S(0.003)
Gray Level Difference Statistics (GLDS)			
Entropy	S(0.02), S(0.04)	S(0.001), S(0.001)	S(0.002), S(0.002)
Contrast	S(0.01), S(0.01)	S(0.001), S(0.001)	S(0.0001), S(0.0001)
Neighborhood Gray Tone Difference Matrix (NGTDM)			
Coarseness	S(0.002), S(0.002)	S(0.002), S(0.002)	S(0.001), S(0.001)
Contrast	S(0.003), S(0.001)	S(0.002), S(0.003)	S(0.001), S(0.001)
Statistical Feature Matrix (SFM)			
Periodicity	S(0.001), S(0.001)	S(0.001), S(0.001)	S(0.001), S(0.001)
Roughness	S(0.001), S(0.001)	S(0.001), S(0.001)	S(0.001), S(0.001)
Laws Texture Energy Measures (LTEM)			
LL	S(0.002), S(0.002)	S(0.001), S(0.001)	S(0.001), S(0.001)
SS	S(0.001), S(0.001)	S(0.001), S(0.001)	S(0.003), S(0.004)
Fractal Dimension Analysis (FDTA)			
H1	S(0.002), S(0.002)	S(0.004), S(0.003)	S(0.002), S(0.004)

N, A, S: Normal, asymptomatic and symptomatic group of subjects, GSM: Gray-scale median, STD: Standard Deviation.

videos from the three different groups investigated in this study (N, A, S). The plaque GSM and contrast were higher for systole than diastole for the N, A and S groups, whereas the reverse applies for entropy (see also Fig. 3 for GSM). Table 2 also shows the %CV for each texture feature. For the %CV, it is shown that the higher variation was observed for the A group for the GSM and contrast features. The highest ρ, was found for the texture feature GSM versus the other features for the different groups studied. It is also shown that ρ, was higher for the A-S group for both systole and diastole when compared with the N-S and N-A groups indicating a stronger relation of the features extracted from the A and S groups.

Table 3 illustrates the statistical analysis between the different groups investigated (N, A, S) for the texture features presented in Table 2 for the systolic and diastolic states. Most of the features are shown to be significantly different for both systole and diastole and thus they might be used to separate the three different groups (N, A, S).

TABLE 4. Atherosclerotic carotid video plaque texture classification evaluation results between the A and S groups. SVM models trained and evaluated using 10-fold cross validation, and the RBF kernel with c=1 and gamma=0.01.

Feat.	CC	%CC	%TP	%FP	%Pre.	%Rec.	ROC
All	80/80	100	100	0	100	100	100
SysF	64/80	80	80	20	81	80	80
DiasF	76/80	95	95	5	96	95	95

A: Asymptomatic and S: Symptomatic groups of subjects. CC: Correct classification, TP: True positive, FP: False positive, Pre: Precision = TP/(TP+FP), Rec: Recall = TP/(TP+FN), ROC: Area under the ROC curve. All: All features used (1: SF-GSM_S, 2: SF-GSM_D, 3: SGLDM-Contrast_S, 4: SGLDM Contrast_D, 5: GLDS-Entropy_S, 6: GLDS-Entropy_D). SysF: Only systole features (1, 3, 5, 7), DiasF: Only diastole features (2, 4, 6, 8).

Table 4 illustrates the classification evaluation results for the A vs S models. As shown the SVM classifier could achieve classification rates of up to 100%. This result should be further validated with data from more subjects and videos acquired from different ultrasound equipment.

Figure 2 illustrates line plots for the texture feature variability through the cardiac cycle for the texture features GSM (SF), periodicity (SFM) and entropy (SGLDMr) for a) an N male subject aged 38, b) an A male subject aged 61 and c) an S male subject aged 63. The features were extracted from the segmented IMC (for the N subject) and plaque ROIs (for the A and S subjects) as shown in Fig. 1a and Fig. 1b. It is clearly shown that there is an IMC and plaque texture variability per frame throughout the cardiac cycle. However, no distinct patterns could be identified (see also Table 2).

Figure 3 presents box plots for the texture feature GSM (SF) for the N, A and S groups for all subjects investigated for the systolic and diastolic states, showing the same trend as in Table 2.

IV. DISCUSSION

The objective of this paper was to investigate texture feature variability in ultrasound video of the carotid artery during the cardiac cycle in an attempt to define new discriminatory biomarkers of the vulnerable plaque. More specifically, in the present work, 120 longitudinal ultrasound videos, acquired from 40 N, 40 A and 40 S subjects were investigated. The videos were intensity normalized and despeckled, and the IMC (from the N subjects) and the atherosclerotic carotid plaques (from the A and S subjects) were segmented from each video, in order to extract the M-mode image, and the texture features associated with the cardiac states of systole and diastole. Classification models were then developed to differentiate between A and S subjects using plaque texture variability features. As documented in Table 1, to the best

of our knowledge, there is no similar study published in the literature so that the findings can be compared.

The main results of this study can be summarized as follows:

Texture features varied significantly throughout the cardiac cycle with significant differences identified between the systolic and diastolic cardiac states. These variations correspond to plaque deformation and compression and the pulse pressure in the case of the IMC for the N group and the plaque for the A and S groups. It should be clarified that it is not the variation between diastole and systole itself, but the variability between A and S subjects for both systolic and diastolic features.

GSM was significantly higher at cardiac systole versus diastole for the N, A and S groups investigated. GSM was higher at systole and lower at diastole for the A group when compared to the N group. GSM then dropped for both systole and diastole for the S group when compared to the A group. Moreover, the gap between systole and diastole is higher for the A group when compared to the S group. In an atherosclerotic carotid plaque image analysis study, performed by our group, carotid plaque GSM was higher for the A group when compared to the S group [5].

Plaque texture features extracted during the cardiac cycle at the systolic and diastolic states can be used to discriminate between A and S subjects successfully as demonstrated via SVM classification models. The combination of systolic and diastolic features yields better performance than those alone.

In addition, the following secondary results can be summarized as follows:

Contrast was significantly higher at cardiac systole versus diastole for the N, A and S groups. For the three different contrast features computed (SGLDM, GLDS and NGTDM) there were significant differences for both systole and diastole when comparing N vs A, N vs S and A vs S. In plaque image analysis SGLDM contrast was higher for the A group when compared to the S group [5] as is the case in this study as well.

Entropy is a measure of the randomness of the image. Entropy was significantly lower at cardiac systole versus diastole for the N, A, and S groups. Significantly higher entropy values at systole were obtained for the S group when compared to the A and N groups. In plaque image analysis (where the images were only normalized and not despeckled as in this study), the reverse trend was identified, i.e. entropy was lower for the S group when compared to the A group [5].

No distinct variability patterns were recorded between the cardiac systolic and diastolic states in spite of the estimated significant statistical differences for several texture features. GSM %CV were slightly higher for the A group when compared to the N and S groups.

There are very few other studies reported in the literature [4], [8], [9], [26] that investigated the variability of the texture features within the cardiac cycle. More specifically, in [9], where the variability of the GSM in 27 carotid artery ultrasound videos (from 19 S subjects with stenosis in the range of 10%-80%) was investigated, an in frame by frame

intensity normalization procedure was also applied in order to reduce the interframe variations. The plaque GSM over all frames on the original videos ranged between 26 and 112 (mean 47, %CV=2.9%) versus, the range of 24 and 96 (mean 46, %CV=2.6%) on the intensity normalized videos. Smaller variations in GSM variability after image normalization were also observed in this study in agreement with the originally proposed paper [13]. Similar findings were also documented by the same group in [8].

It was also shown in [8] and [9] in agreement with the present study, that the GSM of the carotid artery varies throughout the cardiac cycle and that GSM of the plaque may be used as a predictor index for cardiovascular events. It was concluded in [9] that these variations may affect the reproducibility of studies and that these may have implications for the use of the GSM as a predictor of CVD [9]. It should be furthermore noted that in [9], Kanber *et al.* [9] studied periodical variations of GSM and plaque area. They found that the deformation or the compression of the plaque under pulse pressure might cause changes in the measured plaque GSM and cross-sectional area, where periodical variations were observed. It was also reported that periodic variations in the scan plane location and orientation, which are due to out-of-plane plaque, patient or probe motion could also cause such periodic (cyclic) variations. In our study, we measured texture feature variations at two different distinct states that represent cardiac diastole and systole.

It was also previously reported in [26] as well as more recently in [4], that differences in contrast were observed between wall and plaque shoulder, rather than between wall and plaque which indicates the importance of this arterial area. Contrast differences were more pronounced at systole, suggesting that texture properties should be studied at specific instants of the cardiac cycle, as is also reported in the present study (see Table 2, and Table 3). These findings suggest that texture variability along the atherosclerotic wall, which may be indicative of tissue discontinuities, and proneness to rupture, can be quantitatively described with texture indices and reveal valuable morphological phenomena of the vulnerable tissue [4]. In another study [27], a significant monotonic association between motion and texture features of symptomatic atherosclerotic carotid plaques was found. More specifically, it was observed that the contrast of the plaque and the GSM decreases, which also implies that heterogeneous material composition of the plaque reduces its movement in both lateral and longitudinal directions.

In [28], a review study for the current state of research on the association between ultrasound-derived echogenicity indices and blood parameters indicative of carotid plaque stability and activity was presented. It was shown that very limited available data as well as findings were available. Biomarkers were studied such as those related to oxidative stress, lipoproteins and diabetes/insulin resistance which are associated with echolucent plaques. The biomarkers adipokines are associated with echogenic plaques. It was furthermore shown that biomarkers of inflammation and

coagulation have not exhibited any conclusive relationship with plaque echogenicity, and it is not possible to come to any conclusion regarding calcification-, apoptosis- and neo-angiogenesis-related parameters because of the extremely limited bibliographic data.

There are also some limitations for the present study which are summarized below. Cases of plaque type I and type V [13], [29] were not considered for segmentation. If the plaque is of type I, borders are not very visible. Plaques of type V produce acoustic shadowing and the plaque is also not visible well [29]. However, there are also inherent difficulties for segmentation of the carotid videos and the corresponding plaques that arise not only from the use of different protocols but also due to differences in anatomy as well as to the extent of the atherosclerosis and plaque presence. There were about 2% of the cases where the final state diagrams did not produce correctly. Additionally, the study should be applied further on a larger sample of videos, a task which is currently undertaken by our group.

The variations found in the plaque for almost all texture features may be due to a number of different factors. While changes to the acquisition settings during a single acquisition would not be expected, changes in the plaque texture features may occur if the distance between the plaque and the transducer head changed during an acquisition. Patient or probe motion may also change the location and orientation of the scan plane with respect to the plaque being imaged, affecting both the measured texture features and the observed cross-sectional area. These are likely to be significant contributors to the variations seen in the texture feature variations found in this study. Deformation or compression of the plaque under the pulse pressure may also cause changes in the measured plaque features. Other factors which could cause texture variations may include unclear plaque boundaries (bad video quality and speckle noise), which may cause fluctuations in the plaque boundaries. However, the pre-processing (normalization and despeckle filtering) used in this study significantly lowers these fluctuations.

V. CONCLUDING REMARKS

It is shown in this study that texture features extracted from the IMC and plaque of the carotid artery videos during the cardiac cycle differ significantly between cardiac systole and diastole. The combination of systolic and diastolic features can be used to differentiate between the asymptomatic and symptomatic groups. However, the results of this study should be examined further and validated on a larger number of subjects, so that concrete conclusions can be drawn for the texture feature variability throughout the cardiac cycle and how this is connected with the progression of CVD.

Future work will investigate the possible incorporation of the proposed system into a computer aided diagnostic system that supports texture variability video analysis of the segmented plaque, providing an automated system for the early diagnosis and the assessment of the risk of stroke. The association of texture and motion features as well as of

stress and strain as it was documented in [27], with the results of histological examination will also be a challenging future perspective in this line of work.

REFERENCES

[1] X. Cai *et al.*, "The comparison of tissue vibration signal extraction algorithms in shearwave dispersion ultrasound vibrometry," in *Proc. 1st Global Conf. Biomed. Eng., 9th Asian–Pacific Conf. Med. Biol. Eng.*, vol. 47. 2011, pp. 162–164.

[2] U. Baber *et al.*, "Prevalence, impact, and predictive value of detecting subclinical coronary and carotid atherosclerosis in asymptomatic adults: The BioImage study," *J. Amer. College Cardiol.*, vol. 65, pp. 1065–1074, Mar. 2015.

[3] A. Gupta and R. S. Marshall, "Moving beyond luminal stenosis: Imaging strategies for stroke prevention in asymptomatic carotid stenosis," *Cerebrovascular Diseases*, vol. 39, pp. 253–261, Jun. 2015.

[4] S. Golemati, S. Lehareas, N. N. Tsiaparas, K. S. Nikita, A. Chatziioannou, and D. N. Perrea, "Ultrasound-image-based texture variability along the carotid artery wall in asymptomatic subjects with low and high stenosis degrees: Unveiling morphological phenomena of the vulnerable tissue," *Phys. Procedia*, vol. 70, no. 1, pp. 1208–1211, 2015.

[5] C. I. Christodoulou, C. S. Pattichis, M. Pantziaris, and A. Nicolaides, "Texture-based classification of atherosclerotic carotid plaques," *IEEE Trans. Med. Imag.*, vol. 22, no. 7, pp. 902–912, Jul. 2003.

[6] E. C. Kyriacou *et al.*, "Prediction of high-risk asymptomatic carotid plaques based on ultrasonic image features," *IEEE Trans. Inf. Technol. Biomed.*, vol. 16, no. 5, pp. 966–973, Sep. 2012.

[7] S. K. Kakkos *et al.*, "Computerized texture analysis of carotid plaque ultrasonic images can identify unstable plaques associated with ipsilateral neurological symptoms," *Angiology*, vol. 62, no. 4, pp. 317–328, 2011.

[8] B. Kanber, T. C. Hartshorne, M. A. Horsfield, A. R. Naylor, T. G. Robinson, and K. V. Ramnarine, "Wall motion in the stenotic carotid artery: Association with greyscale plaque characteristics, the degree of stenosis and cerebrovascular symptoms," *Cardiovascular Ultrasound*, vol. 11, no. 33, pp. 1–11, 2013.

[9] B. Kanber, T. C. Hartshorne, M. A. Horsfield, A. R. Naylor, T. G. Robinson, and K. V. Ramnarine, "Dynamic variations in the ultrasound greyscale median of carotid artery plaques," *Cardiovascular Ultrasound*, vol. 11, p. 21, Jun. 2013.

[10] C. P. Loizou, S. Petroudi, C. S. Pattichis, M. Pantziaris, and A. N. Nicolaides, "An integrated system for the segmentation of atherosclerotic carotid plaque ultrasound video," *IEEE Trans. Ultrason., Ferroelect., Freq. Control*, vol. 61, no. 1, pp. 86–101, Jan. 2014.

[11] C. P. Loizou, M. Pantziarís, A. N. Nicolaides, and C. S. Pattichis, "Atherosclerotic carotid plaque texture variability in ultrasound video," in *Proc. 6th Eur. Conf. Int. Fed. Med. Biol. Eng. (MBEC)*, vol. 45. Dubrovnik, Croatia, Sep. 2014, pp. 176–179.

[12] N. Soulis, C. P. Loizou, M. Pantziaris, and T. Kasparis, "Texture features variability in ultrasound video of atherosclerotic carotid plaques," in *Proc. 14th Medit. Conf. Med. Biol. Eng. Comput. (Medicon)*, vol. 57. Paphos, Cyprus, Mar./Apr. 2016, pp. 351–354.

[13] T. Elatrozy, A. Nicolaides, T. Tegos, A. Zarka, M. Griffin, and M. Sabetai, "The effect of B-mode ultrasonic image standardisation on the echodensity of symptomatic and asymptomatic carotid bifurcation plaques," *Int. Angiol.*, vol. 17, no. 3, pp. 179–186, 1998.

[14] C. P. Loizou, C. S. Pattichis, C. I. Christodoulou, R. S. H. Istepanian, M. Pantziaris, and A. Nicolaides, "Comparative evaluation of despeckle filtering in ultrasound imaging of the carotid artery," *IEEE Trans. Ultrason., Ferroelect., Freq. Control*, vol. 52, no. 10, pp. 1653–1669, Oct. 2005.

[15] C. P. Loizou and C. S. Pattichis, *Despeckle Filtering for Ultrasound Imaging and Video: Algorithms and Software* (Synthesis Lectures on Algorithms and Software in Engineering), vol. 1, 2nd ed. San Rafael, CA, USA: Morgan & Claypool, 2015, pp. 1–180.

[16] C. P. Loizou *et al.*, "Despeckle filtering toolbox for medical ultrasound video," *Int. J. Monitor. Surveill. Technol. Res.*, vol. 1, no. 4, pp. 61–79, 2013.

[17] C. P. Loizou, A. Nicolaides, N. Georghiou, M. Griffin, E. Kyriacou, and C. S. Pattichis, "A comparison of ultrasound intima-media thickness measurements of the left and right common carotid artery," *IEEE J. Transl. Eng. Health Med.*, vol. 3, 2015, Art. no. 1900410.

[18] C. P. Loizou, M. Pantziaris, M. S. Pattichis, E. Kyriacou, and C. S. Pattichis, "Ultrasound image texture analysis of the intima and media layers of the common carotid artery and its correlation with age and gender," *Comput. Med. Imag. Graph.*, vol. 33, no. 4, pp. 317–324, 2009.

[19] R. M. Haralick, K. Shanmugam, and I. Dinstein, "Textural features for image classification," *IEEE Trans. Syst., Man, Cybern.*, vol. SMC-3, no. 6, pp. 610–621, Nov. 1973.

[20] J. S. Weszka, C. R. Dyer, and A. Rosenfeld, "A comparative study of texture measures for terrain classification," *IEEE Trans. Syst., Man, Cybern.*, vol. SMC-6, no. 4, pp. 269–285, Apr. 1976.

[21] M. Amadasun and R. King, "Textural features corresponding to textural properties," *IEEE Trans. Syst., Man, Cybern.*, vol. 19, no. 5, pp. 1264–1274, Sep./Oct. 1989.

[22] C.-M. Wu, Y.-C. Chen, and K.-S. Hsieh, "Texture features for classification of ultrasonic liver images," *IEEE Trans. Med. Imag.*, vol. 11, no. 2, pp. 141–152, Jun. 1992.

[23] C. P. Loizou, C. Theofanous, M. Pantziaris, and T. Kasparis, "Despeckle filtering software toolbox for ultrasound imaging of the common carotid artery," *Comput. Methods Programs Biomed.*, vol. 114, no. 1, pp. 109–124, 2014.

[24] University of Waikato. (2016). *Weka 3.8 Workbench—Waikato Environment for Knowledge Analysis*. [Online]. Available: http://www.cs.waikato.ac.nz/ml/index.html

[25] V. Vapnik, S. E. Golowich, and A. J. Smola, "Support vector method for function approximation, regression estimation and signal processing," in *Advances in Neural Information Processing Systems*, vol. 9. San Mateo, CA, USA: Morgan Kaufmann, 1997, pp. 281–287.

[26] S. Golemati *et al.*, "Toward recognizing the vulnerable asymptomatic atheromatous plaque from B-mode ultrasound: The importance of the morphology of the plaque shoulder," in *Proc. IEEE Int. Ultrason. Symp.*, vol. 6. Chicago, IL, USA, Sep. 2014, pp. 2390–2393, paper #P1C8.

[27] A. Gastounioti, S. Golemati, and K. S. Nikita, "Computerized analysis of ultrasound images: Potential associations between texture and motion properties of the diseased arterial wall," in *Proc. IEEE Int. Ultrason. Symp.*, Oct. 2012, pp. 691–694.

[28] S. Lechareas, A. E. Yanni, S. Golemati, A. Chatziioannou, and D. Perrea, "Ultrasound and biochemical diagnostic tools for the characterization of vulnerable carotid atherosclerotic plaque," *Ultrasound Med. Biol.*, vol. 42, no. 1, pp. 31–43, 2016.

[29] A. Nicolaides *et al.*, "The asymptomatic carotid stenosis and risk of stroke (ACSRS) study," *Int. Angiol.*, vol. 22, no. 3, pp. 263–272, 2003.

CHRISTOS P. LOIZOU, photograph and biography not available at the time of publication.

CONSTANTINOS S. PATTICHIS, photograph and biography not available at the time of publication.

MARIOS PANTZIARIS, photograph and biography not available at the time of publication.

EFTHYVOULOS KYRIACOU, photograph and biography not available at the time of publication.

ANDREW NICOLAIDES, photograph and biography not available at the time of publication.